HORIBA Scientific

Ground-Based Measurements of Stratospheric Gases Using UV-VIS Spectroscopy

OSD-AN-115

ELEMENTAL ANALYSIS
FLUORESCENCE
GRATINGS & OEM SPECTROMETERS
OPTICAL COMPONENTS
FORENSICS
PARTICLE CHARACTERIZATION
RAMAN
SPECTROSCOPIC ELLIPSOMETRY
SPR IMAGING

Identifying chemical reactions affecting ozone depletion

Introduction

Over the past two decades human activity (namely the release of halogen-containing gases into the atmosphere) has stimulated a decrease in stratospheric ozone abundance. Depletion of the 'ozone layer' is a major concern since ozone shields the Earth's surface from damaging UV radiation. Many chemical reactions pertinent to ozone loss have now been unambiguously identified. However, there remains some discrepancy between results from atmospheric models and observed ozone depletion.

To increase the geographic range and sampling density of ozone observations, a portable ground-based spectrometer system capable of stand-alone measurements of ozone and a number of other trace stratospheric gases was constructed. The instrument has been deployed in the High Arctic to monitor stratospheric composition during the critical period following polar sunrise, when the conditions leading to ozone destruction develop.

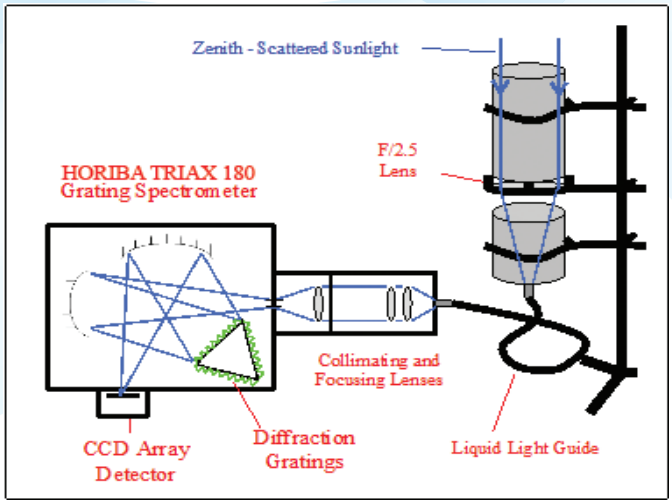

Figure 1. Schematic Diagram of Experimental Set-Up

Methodology

A schematic diagram of the instrumental set-up is shown in Figure 1. In brief, the CCD detector recorded sunlight scattered from the zenith sky throughout the day and differential optical absorption spectroscopy (DOAS) theory was used to retrieve atmospheric column densities of stratospheric gases such as ozone and NO_2. Spectra were acquired in the UV-visible region (typically 336 nm to 570 nm) to take advantage of characteristic absorption features of the gases of interest.

Zenith-scattered sunlight was focused onto a liquid light guide using a fused silica lens. Emergent light from the light guide was then re-focused onto the entrance slit of a HORIBA TRIAX-180 imaging spectrograph. The spectrograph was fitted with an adjustable entrance slit and a triple-grating turret (mounted with diffraction gratings of 400, 600 and 1800 grooves/mm) to ensure flexibility in the resolution and spectral range available. A thermoelectrically cooled HORIBA CCD detector was mounted on the exit focal plane of the spectrograph and provided a focal plane of 30 mm x 12 mm. The CCD was back-illuminated to improve quantum efficiency of signal in the UV region. On-chip binning of each pixel column was performed to maximize signal-to-noise. A CCD array was used rather than a diode array detector to avoid artifacts introduced by signal-dependent dark current and the Fabry-Pérot etalon structure that is inherent in many diode array detectors. All instrumentation was contained in a portable aluminum trunk that was designed for outdoor operation in the

JOBIN YVON Technology

field environment. A heating circuit and temperature monitor were installed in the trunk to maintain a constant ambient temperature.

Spectrometer control and data acquisition were automated using a customized LabVIEW application based on HORIBA's instrument drivers. The system was operated using a laptop computer contained within the box, which resulted in a stand-alone instrument, ideally suited for deployment in remote locations where ozone measurements are sparse. A photograph of the observatory where these measurements were conducted is shown in Figure 2.

Figure 2. Measurements were made at Environment Canada's Arctic Stratospheric Observatory (80° N) located at Eureka, NT, Canada

Results and Discussion

The spectrometer was deployed at mid-latitudes and the High Arctic as a constituent instrument in collaborative field studies of the stratosphere. Here, results are presented from a field study at Environment Canada's Arctic Stratospheric Observatory at Eureka, NT (80.1° N, 86.4° W). Stand-alone measurements were made between March 21 and April 21, 1999. Zenith-sky spectra were recorded at a range of solar elevation angles, with the intensity of scattered sunlight determined by the optical path of solar radiation, and the concentration of absorbing species along that path. The intensity I varies as follows:

$$I_{spec}(\lambda) = F(\lambda) I_o(\lambda) \exp\left[\sum_i \{\sigma_i(\lambda) u_{i,spec}\} + \Delta D_{Ray(\lambda)} + \Delta D_{Mie(\lambda)} \right]$$

where:

- $I_{spec}(\lambda)$ = intensity of zenith-sky spectrum
- $F(\lambda)$ = instrument function
- $I_0(\lambda)$ = solar (Fraunhofer) spectrum
- $\sigma_i(\lambda)$ = absorption cross-section of absorbing species i
- μ_i = atmospheric slant column amount of absorber i
- $OD_{Ray(\lambda)}$ = optical depth due to Rayleigh (molecular) scattering, cross-section known
- $OD_{Mie(\lambda)}$ = optical depth due to Mie (aerosol) scattering, varies as a smooth function of λ

To remove $F(\lambda)$, $I_0(\lambda)$ and broadly varying features such as Mie scattering, a differential spectrum was obtained via a 3-step series. Firstly, a spectrum taken at low solar elevation (twilight) was ratioed to a reference spectrum recorded at a high elevation angle (noon). Secondly, the natural log of the differential spectrum was taken to convert absorption measurements into optical depths. Finally, a polynomial was fitted to remove those absorption and scattering features that vary smoothly with wavelength. The differential spectrum is described below:

$$-\ln\left[\frac{I_{spec}(\lambda)}{I_{ref}(\lambda)}\right] = \sum_i \sigma_i(\lambda)\{u_{i,spec} - u_{i,ref}\} + [\Delta D \quad \sigma_{Ray(\lambda)} + \Delta D \quad \sigma_{Mie(\lambda)}]$$

The line-of-sight amount of each atmospheric absorber was retrieved by fitting differential absorption cross-sections of all relevant gases to the differential zenith-sky spectrum. Ozone, NO_2, O_4, H_2O (BrO and OClO when present in the atmosphere) and Rayleigh cross-sections were fitted using a simultaneous least squares algorithm. A correction for the Ring effect (caused by changes in rotational Raman scattering with solar elevation) was also included. Measured and fitted differential spectra for a typical twilight observation (April 5) during the Eureka campaign of 1999 are illustrated in Figures 3 and 4. The difference between the observed and fitted spectra is shown by the residual structure. A good indication of the quality of our results is the small magnitude of the residual structure compared with the observed spectra.

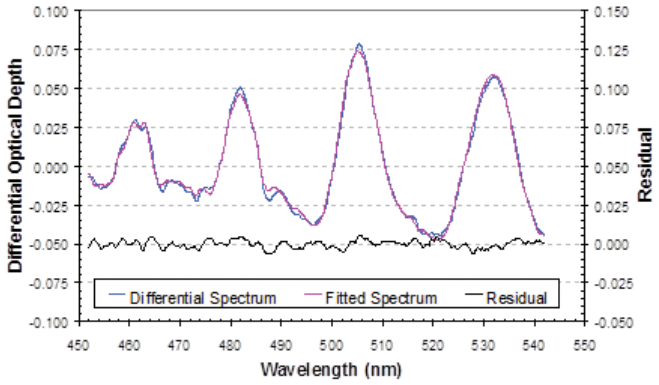

Figure 3: Observed and Fitted Optical Depths in Ozone Wavelength Region

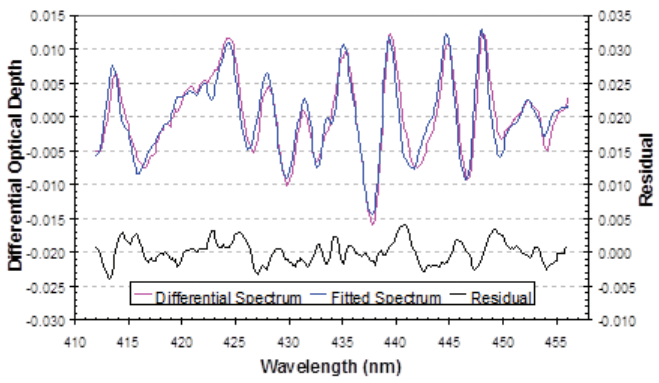

Figure 4: Observed and Fitted Optical Depths in NO_2 Wavelength Region

Line-of-sight amounts of each absorber were converted to vertical column amounts by comparison with a model simulating the transfer of radiation through the atmosphere and associated photon pathlengths through a range of solar elevation angles. Our ozone measurements were compared with satellite observations made using the Total Ozone Mapping Spectrometer (TOMS) - as shown in Figure 5. The good inter-instrument agreement provides some degree of validation for the measurements made using our new system. Ozone column measurements made using four different instruments during a field campaign at Vanscoy, SK, Canada in August 1998, agreed to within 5 %. Estimated errors on our measurements are < 5 % for ozone and 10-12 % for NO_2.

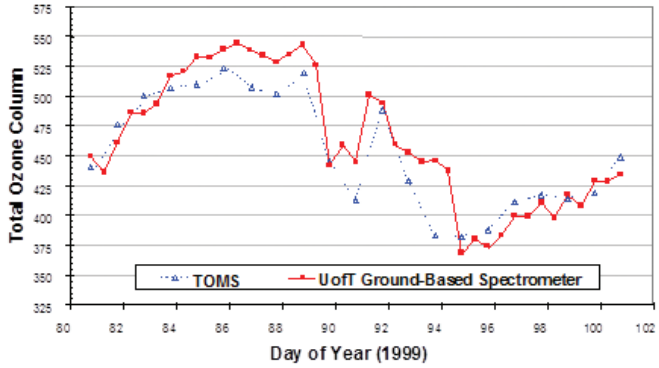

Figure 5. Ozone measurements over Eureka during Spring 1999

The ground-based spectrometer was re-deployed at Eureka for an extended measurement campaign in the spring of 2000. Data from both field studies is currently being analyzed and modeled in an attempt to better understand the science behind ozone loss. Further Arctic campaigns are planned in order to monitor future changes in the abundance of ozone and the species associated with ozone depletion.

Acknowledgements

This experimental work was done by Matt Bassford and Kimberly Strong at the Department of Physics, University of Toronto, Toronto, ON, Canada. More details on the research activities carried out by the atmospheric physics division can be found at http://www.atmosp.physics.utoronto.ca/people/strong/strong.html. Funding for the instrumentation and fieldwork was provided by the Natural Sciences and Engineering Research Council of Canada. The authors are also grateful to Environment Canada for the use of their facilities at Eureka. http://acebox.uwaterloo.ca/eureka/